

Resolution and Sensitivity as a Function of Energy and Incident Geometry for Germanium Detectors

Ronald M. Keyser

ORTEC

801 South Illinois Avenue

Oak Ridge, TN 37831

Abstract

The use of modeling programs such as MCNP to predict the response of HPGe detectors is increasing in importance. Accurate simulation of germanium detectors to incident gamma rays relies on knowledge of the performance of the detector in different detector-source geometries. Two important performance parameters are the resolution and sensitivity. The resolution is the FWHM and FW.1M/FWHM ratio. The IEEE 325-1996 standard only specifies the FWHM measurement at one geometry and two energies. Nearly all measurements are made in a different geometry and at other energies. Other investigators [1,2], have shown that the sensitivity and resolution change with position of the incident gamma ray on the front of the detector. Such variability has possible implications for the accuracy of peak shape and area determination, since the calibration is potentially a function of angle of incidence. To quantify the sensitivity and resolution variation as a function of energy and point of incidence, measurements have been made on several coaxial detectors of various crystal types and sizes in different source-detector geometries. The full-energy peaks from 59 keV to 2.6 MeV were used. The detectors were placed in a low-background shield to reduce any contribution from external sources. None of the detectors tested was a low-background type. The sources used were an ^{241}Am source, ^{60}Co source and a natural thorium oxide sample. The ^{241}Am 59 keV gamma rays were collimated by a 2 cm thick, 1 mm diameter lead collimator. Several gamma rays from the thorium source were used and collimated by a 10 cm thick and 2 mm diameter tungsten collimator. These collimated sources were used to collect spectra for the incident beam on the front and sides of the detectors. The peak widths were calculated using the methods outlined in IEEE 325-1996. Data are presented to show that the peak shape and sensitivity change with incident beam position and full peak energy.

Introduction

In a previous paper [3], it was shown that the normal specifications for a germanium gamma-ray detector are not sufficient to determine the appropriateness of the detector for a specific application. Gehrke, et al, also demonstrated this, but also gave measurement results showing that even more details of the detector are needed. Specifically, these details are needed when the performance of the detector is to be predicted by modeling programs. In this paper, the results of measurements similar to those of Gehrke and Metzgers, but on different types of detectors will be shown. The measurements are scans of the detectors using small-diameter, well-collimated beams of different energy gamma rays. These scans show the sensitivity as a function of incident position as well as the peak shape as a function of incident position.

Experimental Setup

The sources used were ^{241}Am , ^{60}Co and natural thorium oxide. The ^{241}Am and ^{60}Co are point sources and the thorium oxide is bulk powder.

The ^{241}Am source was collimated to a 1 mm diameter beam by a 3 cm long by 17 mm diameter lead collimator as shown in Fig. 1.

The ^{60}Co source was collimated to a 2 mm diameter beam by a tungsten collimator as shown in Fig. 2. The major part of the collimator is 4 cm long by 6 cm diameter. The off-axis penetration of the 4 cm tungsten by the 1.33 MeV gamma ray is about 1.5% and for 8 cm about 0.02% (3.8% and 0.15% for 2.6 MeV).

The thorium oxide source was placed in the collimator shown in Fig. 2, but the source itself is a cylinder 8 mm diameter by 53 mm long. The cylinder is placed such that the long axis is along the axis of the 2 mm hole in the tungsten.

For the scans across the front of the detector, the sources and collimators were positioned above the endcap at a distance of 1 to 2 cm between the bottom of the collimator and the endcap depending on the detector. The collimator was placed in a plastic carrier that was driven by a lead screw between two guide rails. The motion of the source was parallel to the front of the endcap. The collimator was aligned vertically so that the beam impinged on the detector at right angles.

For the scans down the side of the detector, the sources and collimators were positioned at a distance of 3 to 6 mm from the side of the endcap depending on the detector. The collimators were placed on a platform which was raised and lowered by a screw jack. The motion of the platform was parallel to the long axis of the detector. The collimator was positioned such that the beam impinged on the detector on a radius through the

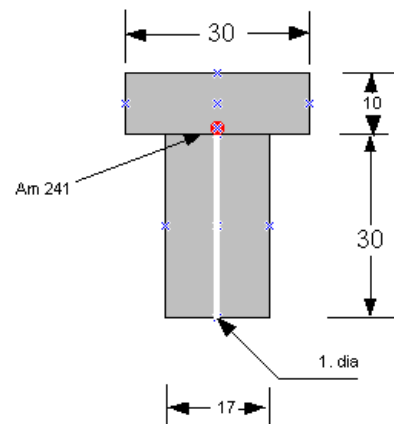


Figure 1 The ^{241}Am source holder

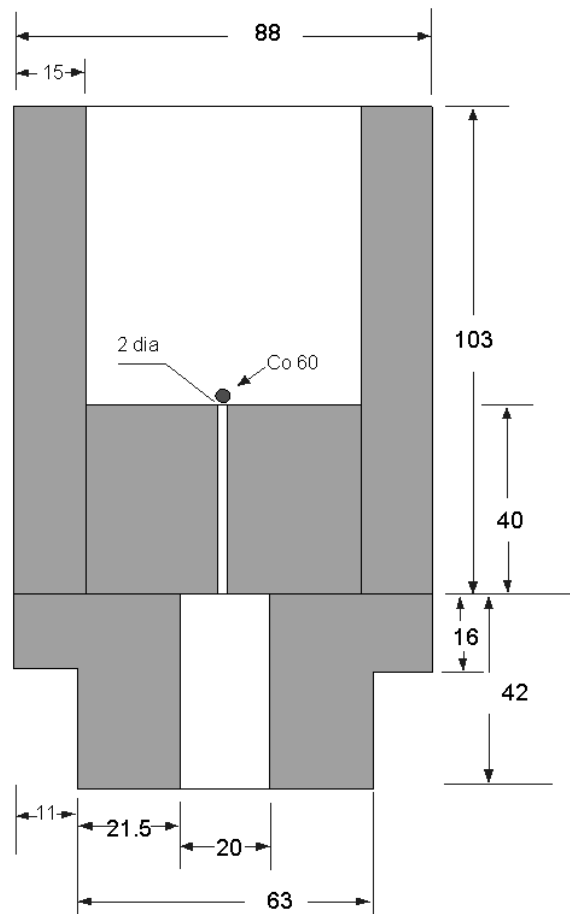


Figure 2 The ^{60}Co collimator

center of the detector.

Figure 3 shows the directions of the scans for the East-West (EW), North-South (NS) and Up-Down (UD).

All of the measurements were taken with the detector in a lead shield. The lead shield walls are 15 cm thick, the bottom is 10 cm thick and the top is 5 cm thick. There was no liner. The main purpose of the shield was to remove any contribution to the peaks of interest especially the 2614 keV peak. The ^{241}Am spectra were typically 300 seconds each. The ^{60}Co were typically 30 minutes each and the thorium spectra were 10 hours each.

None of the sources were calibrated or certified, so it was not possible to calculate absolute efficiencies.

The peak areas and widths were calculated using the methods described in IEEE 325-1996 and IEC 61976-2000.

Discussion

The use of programs such as MCNP and others to calculate the response of a germanium detector to the emissions of a source is increasing. The detailed description of the detector, including the dead layer, is necessary to obtain realistic results from any modeling program. The main details of the detector construction are shown in Fig. 4. As little material as possible is used between the crystal and the outside of the endcap.

In preparation for use in modeling programs, Gehrke measured several detectors. One scan at 238 keV, is shown in Fig. 5. This scan is down the side of a detector. Note that the sensitivity varies due to the copper ring and from an increased dead layer at the bottom. A different detector is shown in Fig. 6. Note the uniform sensitivity in this detector.

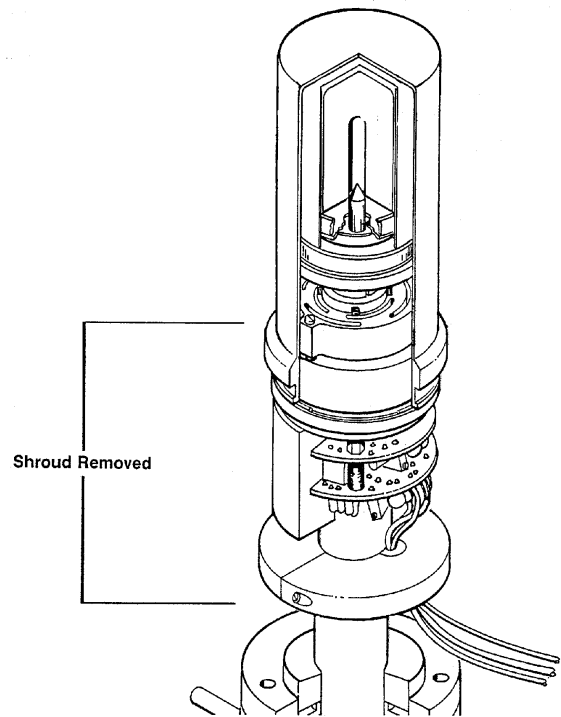
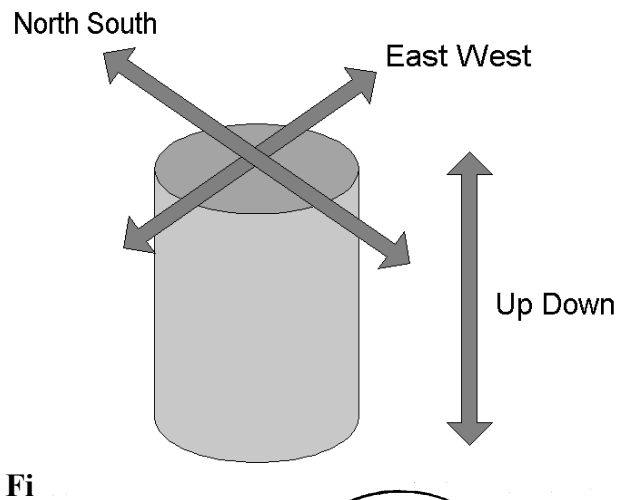


Figure 4 Major detector details

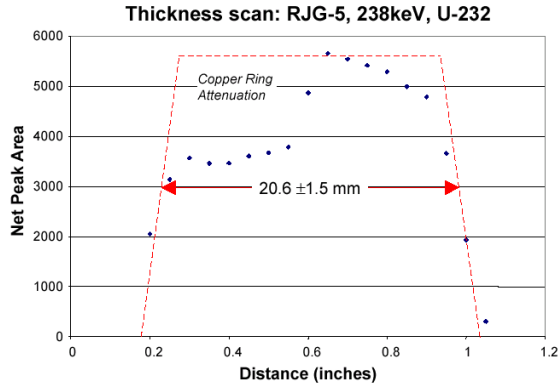


Figure 5 Detector Side Scan Results

Metzger's work involved the use of specially-collimated detectors. The dead layer of the detectors were measured for use in the MCNP program. A highly-collimated ^{241}Am beam was used to measure the germanium dead layer on the detectors. The measurements of a small detector are shown in Fig. 7. This figure shows the relative intensity as a function of position on the front of the endcap for both the East-West and North-South directions. Note the wide variation in peak count rate in the different positions for the incident beam. Also, note that this gamma-ray energy is lower than the gamma-ray energy shown in Figs. 5 and 6, so this measurement is more sensitive to the dead layer.

Metzger's side scan of a large detector is shown in Fig. 8. In this scan he used the same ^{241}Am source along the side of the detector. Note the drop in relative intensity (increase in dead layer) toward the open end (back) of the detector.

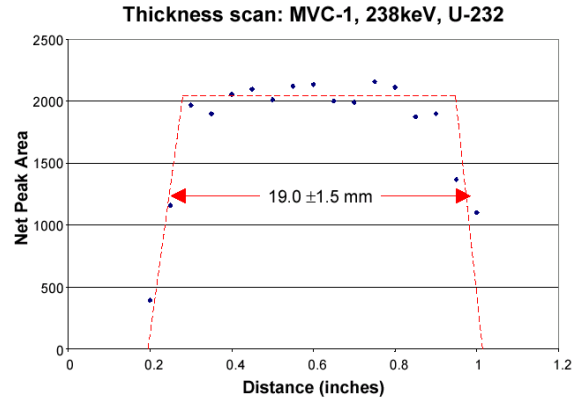


Figure 6 Detector Side Scan Results

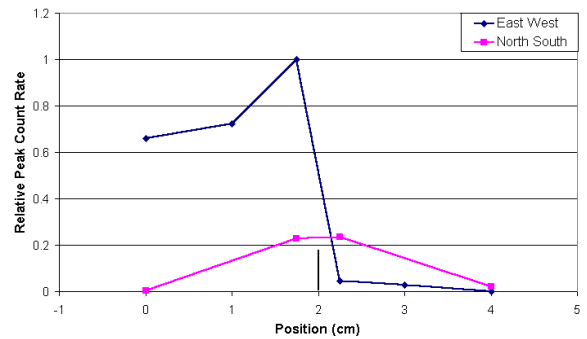


Figure 7 Detector Front Scan Results

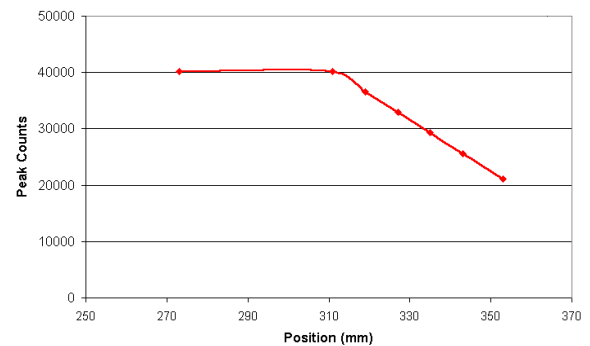


Figure 8 Detector Side Scan Results

Results

The previous works show a large variation in the dead layer over the outer surface of different detectors. This variation could have an impact on the accuracy of the calculated response for the detector.

To study this variation further, several detectors were scanned in similar fashion to the previous work. Both n-type and p-type detectors were used. For the p-type detectors, only large detectors were used as it was expected that these would have the largest variation of the dead layer.

The first detector studied was a GMX (n-type) with dimensions of 60 mm diameter and 60 mm length. The ^{241}Am scan on the front is shown in Fig. 9. The crystal diameter is shown by the black bar.

Another small GMX detector is shown in Figs. 10 and 11. This shows the 59 keV peak area for the East-West scan plotted both left-to-right and right-to-left. In this manner, any differences will easily be seen. Fig. 11 shows the same detector for the North-South scan. Note that both scans are nearly the same, indicating that the crystal has uniform dead layer on the front.

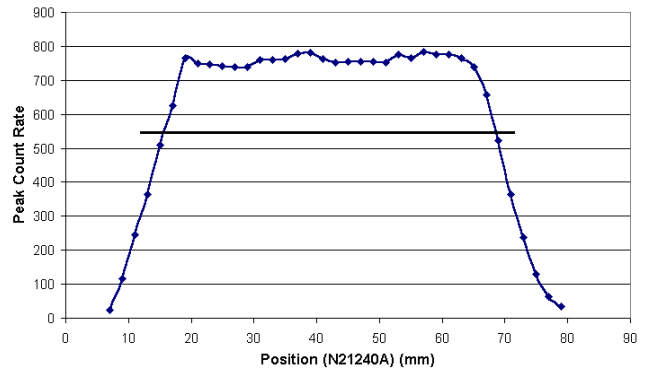


Figure 9 Peak Area vs Position on Front for 59 keV

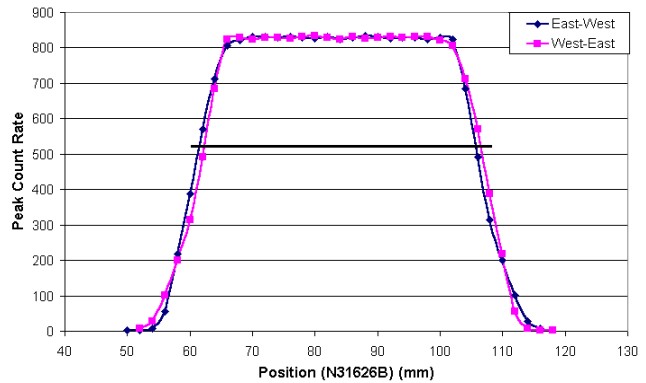


Figure 10 Peak Area vs Position on Front for 59 keV in EW Direction

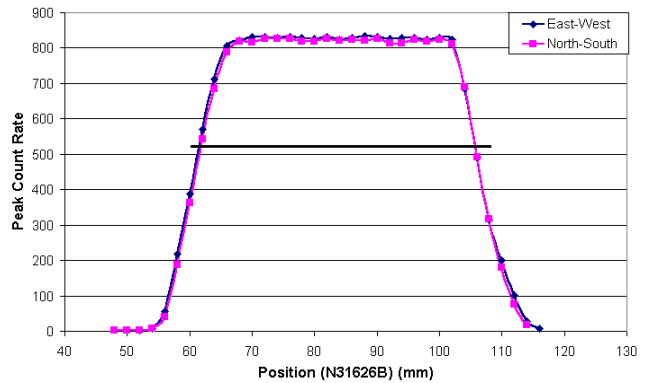


Figure 11 Peak Area vs Position on Front for 59 keV in NS Direction

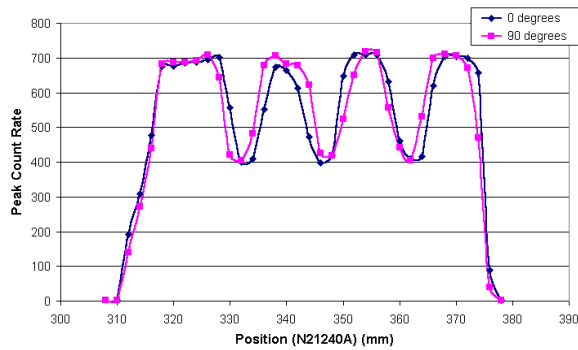


Figure 12 Peak Count Rate at 59 keV vs Position on Side of Detector

The peak area for the scans down the length of the crystal are shown for the first detector in Fig. 12 and for the second in Fig. 13. The second detector is also a GMX and is 48 mm diameter and 53 mm long. Two scans taken at 90° apart are shown.

The intensity of the peak in Fig. 12 shows the three thick regions in the mounting cup of the detector. More importantly, the two scans are nearly the same. The slight variation between the front of the crystal (left side) and the bottom of the crystal in the reduction in count with position is attributed to the increase in material at the bottom of the mounting cup. The peak area in the regions where the cup is thin, show that the dead layer is uniform along the length of the crystal.

Fig. 13 shows the same uniformity of dead layer for another detector.

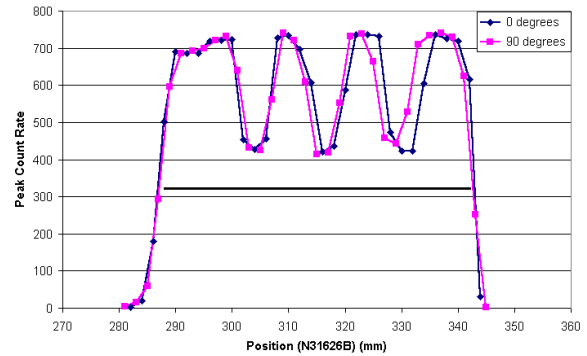


Figure 13 Peak Count Rate at 59 keV vs Position on Side of Detector

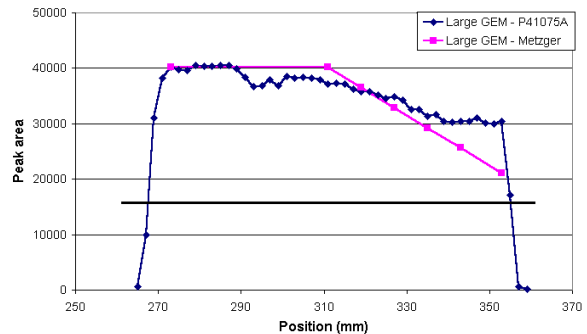


Figure 14 Peak Count Rate at 59 keV vs Position on Side of Detector P41075A

The relative dead layer was also measured for larger GEM detectors. Fig. 14 shows the relative intensity of the 59 keV peak for a scan along the length (UD) of the crystal. For comparison, the results of Ref. 2 for a similar, but not identical, detector are shown. Note that the first thick band is visible, but the second band is obscured by the thickening dead layer. In both of these detectors, the dead layer appears to be constant for a portion of the detector (starting at the closed end or front) and then increasing in thickness from some point on to the bottom of the crystal.

In contrast to these two detectors, Fig. 15 shows a 59 keV scan of a third detector, again of similar length and diameter. In this scan, both the thick bands of the cup can be seen and the dead layer is otherwise nearly

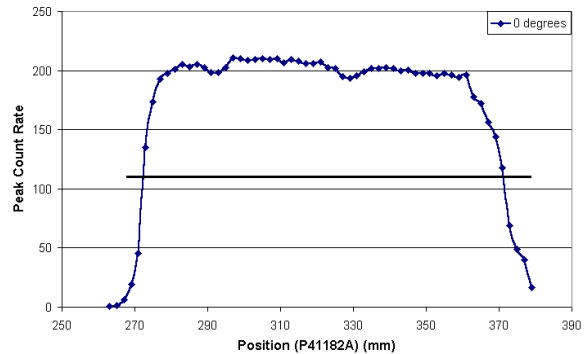


Figure 15 Peak Count Rate at 59 keV vs Position on Side of Detector for P41182A

uniform from front to rear of the crystal.

In addition to the 59 keV scans, the detectors were scanned with a collimated ^{60}Co beam. The scan UD for both 1173 and 1332 keV is shown in Fig. 16. This is the same detector and position as the detector in Fig. 15. The 1173 and 1332 keV UD scan has been plotted UD and DU to show the similarity between the front and rear of the crystal. This plot shows the sensitivity is uniform away from the ends of the crystal.

Fig. 17 shows the same plot for the GEM detector in Fig. 14. The 1173 and 1332 keV UD scan has been plotted UD and DU. Note that the detector is very symmetric top-to-bottom, which is not seen in the 59 keV scan.

Gehrke measured the peak shape for the 2614 keV energy and showed a dependence of the shape with position of the incident beam on the front of the detector. For the measurements here, the peak shape was also calculated. The FWHM, Full-Width-Tenth-Maximum (FW.1M) and Full-Width-Twentyfifth-Maximum (FW.04M) were calculated for each position. For the detector shown in Fig. 14, the resolution for the 2614 peak is shown in Fig. 18.

To further study the effect of the central hole, the resolution was calculated for the ^{60}Co peaks for scans across the front of the detector. The resolution is shown in Fig. 19. Note that this scan shows the same dependence of the FW.1M and FW.04M with front position as seen by Gehrke. The broadening of the peak near the center of the crystal is due to the center hole of the detector. Similar, but smaller variation is seen in the other large GEM detector.

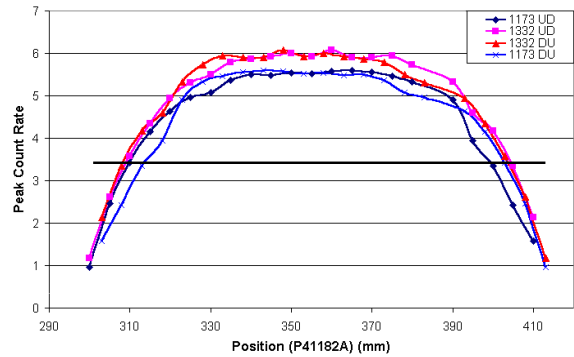


Figure 16 Peak Count Rate at 1173 and 1332 keV vs Position on Side of Detector P41182A

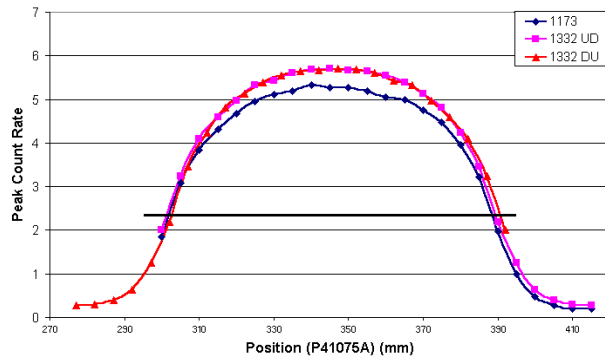


Figure 17 Peak Count Rate at 1173 and 1332 keV vs Position on Side of Detector P41075A

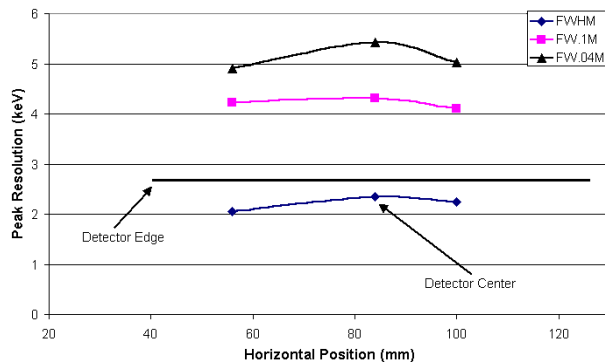


Figure 18 Peak Resolution at 2.6 MeV vs Position on Front of Detector P41075A

Conclusion

The measurements on these several detectors in general support the previous measurements, indicating that the dead layer cannot always be considered to be a uniform thickness on the surface of the crystal. In addition, the dead layer thickness may not be slowly varying with position. However, these measurements also indicate that some detectors do have a uniform dead layer over the surface of the crystal.

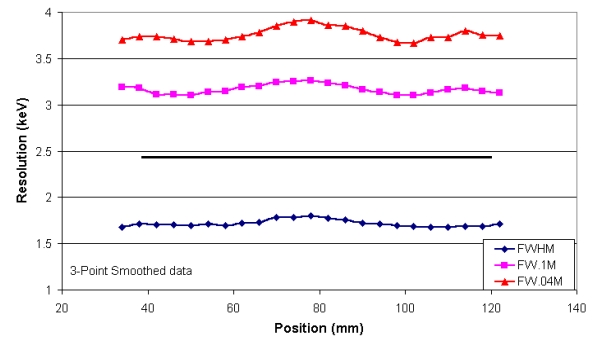


Figure 19 Peak Resolution at 1332 keV vs Position on Front of Detector P41075A

Thus, any model of a detector performance will, of necessity, require a very precise characterization of the exact detector. Future work on other detectors will extend these measurements and compare the MCNP predictions for different assumptions with experimental results.

1. R. J. Gehrke, R. P. Keegan, and P. J. Taylor, "Specifications for Today's Coaxial HPGe Detectors," 2001 ANS Annual Meeting, Milwaukee, WI
2. R. L. Metzger, private communication, see also: R. L. Metzger, K. A. Van Riper, and K. J. Kearfott, "Radionuclide Depth Distribution by Collimated Spectroscopy," 2002 ANS Topical Meeting, Santa Fe, NM
3. R. M. Keyser, T. R. Twomey and P. Sangsingkeow, "Advances in HPGe Detectors For Real-World Applications," Journal of Radioanalytical and Nuclear Chemistry, Vol. 244, No. 3 (2000) 641-647.